Range and Magnitude of the Steric Pressure Between Bilayers Containing Phospholipids with Covalently Attached Poly(ethylene glycol)

A. K. Kenworthy,* K. Hristova,‡ D. Needham,‡ and T. J. McIntosh*

*Department of Cell Biology, Duke University Medical Center, Durham, North Carolina 27710; and ‡Department of Mechanical Engineering and Materials Science, Duke University, Durham, North Carolina 27706 USA

ABSTRACT The interactive properties of liposomes containing phospholipids with covalently attached poly(ethylene glycol) (PEG-lipids) are of interest because such liposomes are being developed as drug delivery vehicles and also are ideal model systems for measuring the properties of surface-grafted polymers. For bilayers containing PEG-lipids with PEG molecular weights of 350, 750, 2000, and 5000, pressure-distance relations have been measured by X-ray diffraction analysis of liposomes subjected to known applied osmotic pressures. The distance between apposing bilayers decreased monotonically with increasing applied pressure for each concentration of a given PEG-lipid. Although for bilayers containing PEG-350 and PEG-750 the contribution of electrostatic repulsion to interbilayer interactions was significant, for bilayers containing PEG-2000 and PEG-5000 the major repulsive pressure between bilayers was a steric pressure due to the attached PEG. The range and magnitude of this steric pressure increased both with increasing PEG-lipid concentration and PEG size, and the extension length of the PEG from the bilayer surface at maximum PEG-lipid concentration depended strongly on the size of the PEG, being less than 35 Å for PEG-750, and about 65 Å for PEG-2000 and 115 Å for PEG-5000. The measured pressure-distance relations have been modeled in terms of current theories (deGennes, 1987; Milner et al., 1988b) for the steric pressure produced by surface-grafted polymers, as modified by us to take into account the effects of polymer polydispersity and the possibility that, at low grafting densities, polymers from apposing bilayers surfaces can interpenetrate or interdigitate. No one theoretical scheme is sufficient to account for all the experimental results. However, for a given pressure regime, PEG-lipid size, and PEG-lipid surface density, the appropriately modified theoretical treatment gives a reasonable fit to the pressure-distance data.

INTRODUCTION

Liposomes containing phospholipids with covalently attached poly(ethylene glycol) (PEG-lipids) are currently being developed for in vivo drug delivery (Klibanov et al., 1990; Blume and Cevc, 1990, 1992; Allen and Hansen, 1991; Lasic et al., 1991; Papahadjopoulos et al., 1991; Gabizon, 1992; Mayhew et al., 1992). A key feature of liposomes containing critical concentrations of specific PEG-lipids is that, when injected into the blood stream, they have long blood circulation times compared with ordinary liposomes (Blume and Cevc, 1990; Klibanov et al., 1990; Papahadjopoulos et al., 1991; Wu et al., 1993). Because of this long circulation time, such PEG-liposomes have the potential to be targeted to specific sites in the body and used as drug delivery vehicles (Mori et al., 1991; Allen et al., 1994).

The relatively long blood circulation time of PEG-lipids is thought to be due to a steric barrier around the liposome provided by the attached PEG (Lasic et al., 1991; Needham and McIntosh, 1991; Woodle et al., 1992b; Woodle and Lasic, 1992). This steric barrier for lipid bilayers containing a PEG-lipid with attached PEG of molecular weight 2000 (PEG-2000) has been measured by two different techniques, an osmotic pressure/x-ray diffraction method (Needham et al., 1992a, b) and a surface force apparatus (Kuhl et al., 1994). These sets of measurements were performed on bilayers containing 0–9 mol % PEG-2000. In the accompanying paper (Kenworthy et al., 1995) we found that, depending on the size of the PEG, as much as 15 mol % PEG-lipid could be incorporated into distearoylphosphatidylcholine (DSPC) bilayers without appreciably modifying the structure of the DSPC bilayer. In this paper, we use x-ray diffraction analysis of osmotically stressed multilamellar liposomes to obtain pressure-distance relations for DSPC:PEG-lipid bilayers containing 0–15 mol % PEG-lipids with PEG molecular weights of 350, 750, 2000, or 5000 Da. Data sets are also presented for higher PEG-lipid concentrations, where other bilayer phases have been shown to exist (Kenworthy et al., 1995).

The results of our experiments are: 1) compared with previous measurements for the steric pressure produced by PEGs grafted onto solid surfaces (Claesson and Gölander, 1987; Costello et al., 1993) or between PEG-lipid bilayers supported on solid surfaces (Kuhl et al., 1994), 2) modeled in terms of recent theoretical treatments of steric pressures (Alexander, 1977; deGennes, 1987; Milner et al., 1988a, b; Milner, 1991), and 3) correlated with the blood circulation times measured for liposomes containing these same PEG-lipids (Klibanov et al., 1990; Allen et al., 1991; Papahadjopoulos et al., 1991; Woodle et al., 1992b).

Received for publication 17 October 1994 and in final form 9 February 1995.

Address reprint requests to Dr. Thomas J. McIntosh, Department of Cell Biology, Duke University Medical Center, Box 3011, Durham, NC 27710. Tel.: 919-684-8950; Fax: 919-684-3687; E-mail: tom mcintosh@cellbio.duke.edu.

Dr. Kenworthy's present address is Biology Department Johns Hopkins University, 3400 N. Charles St., Baltimore, MD 21218.

Dr. Hristova's present address is Department of Physiology and Biophysics, Medical Sciences I, University of California, Irvine, CA 92717-4560.

0006-3495/95/05/1921/16 $2.00

MATERIALS AND METHODS

Materials

PEG-lipids consisting of distearoylphosphatidylethanolamine with PEG covalently attached to the amine group (*N*-(carbamyl-poly(ethylene glycol) methyl ether)-1,2-distearoyl-*sn*-glycerol-3-phosphoethanolamine) were gifts from Liposome Technology, Inc. (Menlo Park, CA). The PEG-lipids used in these studies contained PEGs with average molecular weights of 350, 750, 2000, and 5000, and are subsequently referred to as PEG-350, PEG-750, PEG-2000, and PEG-5000, respectively. For some experiments (where indicated), PEG-2000 and PEG-5000 (>98% purity) were also obtained from Avanti Polar Lipids (Alabaster, AL). These lipids are referred to as Avanti PEG-2000 and Avanti PEG-5000. Typical values for the weight-average molecular weight (M_w) and the number-average molecular weight (M_n) for PEG chains used in the synthesis of PEG-lipids were provided by Union Carbide (South Charleston, WV). They are PEG 750, M_w = 739, M_n = 670; PEG 2000, M_w = 2211, M_n = 2059; and PEG 5000, M_w = 5581, M_n = 5394.

Distearoylphosphatidylcholine (DSPC) was obtained from Avanti Polar Lipids and dextran with an average molecular weight of 503,000 Da and poly(vinylpyrrolidone) (PVP) with an average molecular weight of 40,000 Da were purchased from Sigma Chemical Co. (St. Louis, MO.).

Osmotic stress method

To measure the range and magnitude of the repulsive pressure between bilayers, an "osmotic stress" technique was used whereby known osmotic pressures are applied to multiwalled liposomes and the distance between bilayers at each applied pressure is measured by x-ray diffraction analysis (LeNeveu et al., 1977; Parsegian et al., 1979; McIntosh and Simon, 1986; McIntosh et al., 1989a). At equilibrium, the total repulsive pressure between apposing bilayers is balanced by the sum of the attractive van der Waals pressure and the applied osmotic pressure. Under conditions where the applied pressure is significantly larger than the van der Waals pressure, the total repulsive pressure between bilayers can be equated to the osmotic pressure (LeNeveu et al., 1977). Therefore this method provides the total repulsive pressure between bilayers as a function of distance between bilayers.

The osmotic stress was applied to the liposomes by equilibrating them in solutions containing the large, neutral polymers dextran or PVP. Osmotic pressures of dextran and PVP solutions as a function of polymer concentration have previously been measured (Vink, 1971; Parsegian et al., 1986; McIntosh et al., 1989b). A major assumption in the osmotic stress technique is that stressing polymer is too large to enter the lipid multilayers. We argue that this assumption is valid for DSPC:PEG-liposomes with the dextran and PVP solutions we have used, since these liposomes gave identical x-ray repeat periods in solutions containing either PVP (40,000 Da) or dextran (500,000 Da) that produced equivalent measured osmotic pressures. This indicates that stressing polymers of very different sizes produced the same effective osmotic pressure on the DSPC:PEG-lipid multilayers.

Sample preparations

Mixtures of DSPC and PEG-lipids were co-dissolved in chloroform. After the chloroform was removed by rotary evaporation, excess amounts (at least 90% by weight) of solutions of dextran or PVP in 100 mM NaCl, 20 mM HEPES at pH 7.0 were added to the dry lipid samples. To insure complete hydration and equilibration of salt across the multibilayers, the lipid suspensions were incubated for several hours at 70°C (above the main phase transition temperature of both DSPC and the PEG-lipids), periodically vortexed, and cycled through the main phase transition temperature at least three times. Long equilibration times at room temperature (up to 2 weeks) did not appreciably change the lamellar repeat period.

X-ray diffraction

X-ray diffraction patterns were recorded from DSPC:PEG-lipid specimens by the same procedures described in the accompanying paper (Kenworthy et al., 1995). Electron density profiles, $\rho(x)$, on a relative electron density scale were calculated from

$$\rho(x) = (2/d)\sum \exp\{i\phi(h)\} \cdot F(h) \cdot \cos(2\pi xh/d) \quad (1)$$

where $F(h)$ is the x-ray structure amplitude, x is the distance from the center of the bilayer, d is the lamellar repeat period, $\phi(h)$ is the phase angle for order h, and the sum is over h. The phase angles, $\phi(h)$, for these DSPC:PEG-lipid bilayers have been determined previously (Kenworthy et al., 1995). Profiles presented in this paper are at a resolution of $d/2h_{max} \approx 8$ Å.

RESULTS

X-ray diffraction

For all DSPC:PEG-lipid suspensions described here, in 0.5–20% dextran solutions (corresponding to applied osmotic pressures of 8.85×10^2 to 1.03×10^6 dyn/cm^2) or 6–46% PVP solutions (corresponding to applied osmotic pressures of 1.06×10^5 to 1.69×10^7 dyn/cm^2), the x-ray diffraction patterns contained one or two wide-angle reflections and several low-angle reflections that indexed as orders of a lamellar repeat, d. For dextran and PVP solutions giving equivalent osmotic pressure, the same wide-angle and low-angle diffraction patterns were observed.

Wide-angle diffraction

The wide-angle reflections for DSPC:PEG-lipid suspensions with no applied pressure or small applied pressures ($< 3.6 \times 10^5$ dyn/cm^2) have been presented in the accompanying paper (Kenworthy et al., 1995). For all DSPC:PEG-lipid specimens described here, the spacings of the wide-angle reflections were not changed by the application of osmotic pressures in the range of 2×10^4 to 1.0×10^7 dyn/cm^2. This indicates that the lipid hydrocarbon chain packing was not changed appreciably over this range of applied pressures.

Low-angle diffraction and pressure-distance measurements

Fig. 1, *A–F* show plots of the logarithm of applied pressure (log P) versus the lamellar repeat period (d) for the DSPC:PEG-lipid suspensions. For each DSPC:PEG-lipid mixture, the lamellar repeat period decreased monotonically with increasing applied pressure for $2 \times 10^3 < P < 1.6 \times 10^6$ dyn/cm^2 ($3.3 < \log P < 6.2$). Within this range of applied pressures, the pressure-repeat period relations were strong functions of both the molecular weight of the PEG and the concentration of PEG-lipid (Fig. 1). In particular, for a given PEG molecular weight at a given applied pressure, the repeat period increased monotonically with PEG-lipid concentration up to concentrations of about 40 mol % for PEG-350, 10 mol % for PEG-750 (Fig. 1 *B*), 10 mol % for PEG-2000 (Fig. 1 *C*), and 10 mol % for PEG-5000 (Fig. 1 *D*). At higher PEG-lipid concentrations the behavior of the pressure-repeat period curves with increasing PEG-lipid concentration depended on the PEG molecular weight, reflecting underlying differences in the lipid phase of the samples (Kenworthy et al., 1995). For example, at a given applied pressure for dispersions containing PEG-350 (Fig. 1 *A*) the repeat period decreased about

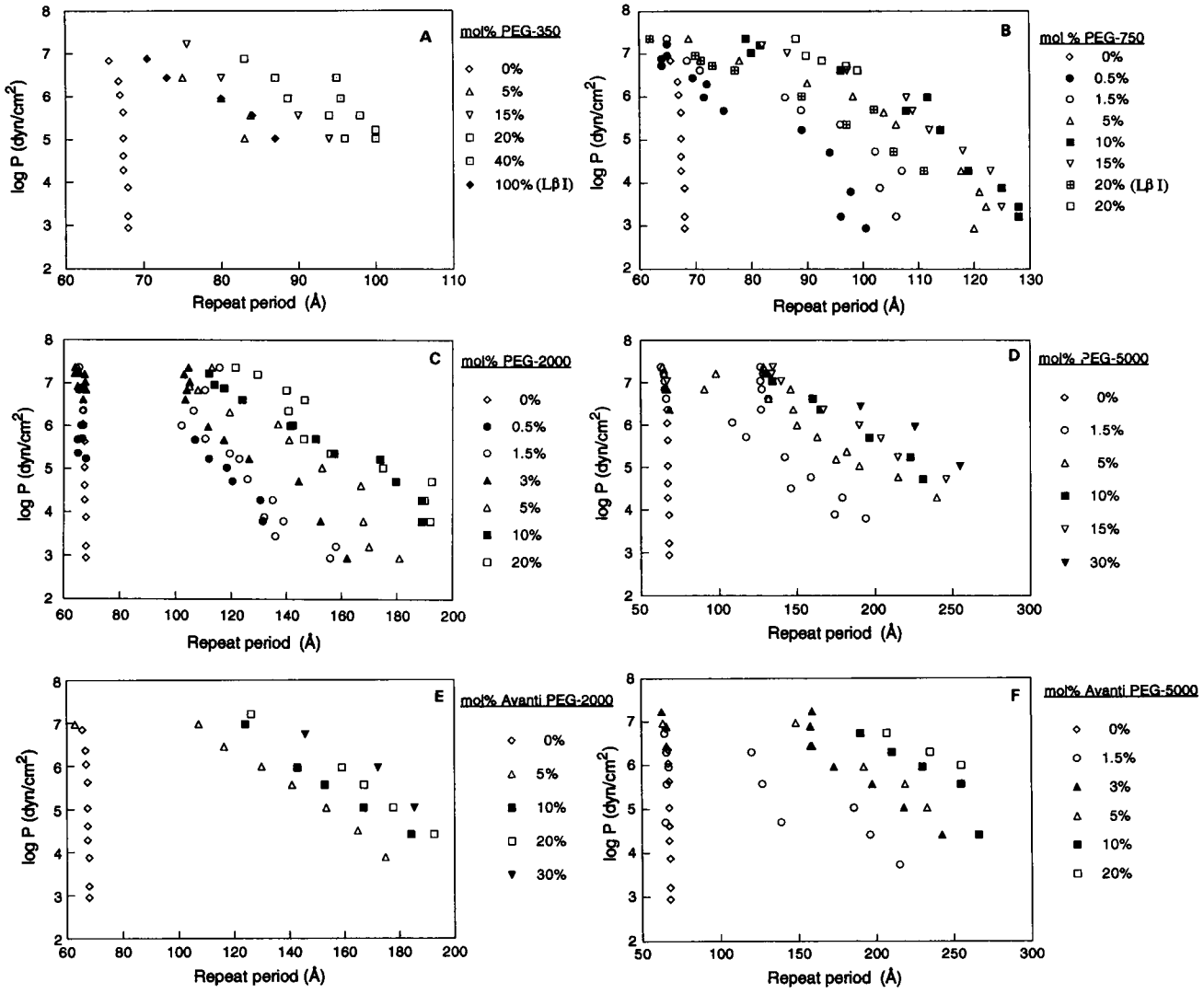

FIGURE 1 Logarithm of applied osmotic pressure (log P) versus lamellar repeat period for DSPC bilayers containing various concentrations of (A) PEG-350, (B) PEG-750, (C) PEG-2000, (D) PEG-5000, (E) Avanti PEG-2000, and (F) Avanti PEG-5000. Data points from bilayers in the interdigitated (LβI) phase are noted in panels (A) and (B). As described in the text, all other points are from bilayers in non-interdigitated phases (Lβ' or Lβ).

15 Å as PEG-lipid concentration was increased from 40 mol % to 100 mol % and for DSPC:PEG-750 dispersions the repeat periods overlapped for 10 and 15 mol % PEG-lipid, and then decreased about 15 Å as the PEG-lipid concentration was increased from 15 to 20 mol % (Fig. 1 B). These observations of decreased repeat periods with increasing PEG-lipid concentrations can be explained by the conversion of the gel bilayer phase from the Lβ' gel phase to the LβI gel bilayer phase with the addition of these PEG-lipids. The width of the bilayer is about 15 Å greater for the Lβ' phase than for the LβI phase (Kenworthy et al., 1995). In the cases of PEG-2000 and PEG-5000, overlapping pressure-distance curves were observed for PEG-lipid concentrations between 10 and 15 mol %. However, the repeat period further increased slightly as the bilayer structure shifted from Lβ' to Lβ with the addition of >15 mol % of Avanti PEG-2000 (Fig. 1 D), PEG-5000 (Fig. 1 E), and Avanti PEG-5000 (Fig. 1 F).

For some DSPC:PEG-lipid mixtures at applied pressures >1.5 × 10^6 dyn/cm^2 (log P > 6.2), two lamellar repeat periods were observed, indicating lipid phase separation had occurred (Fig. 1). For DSPC:PEG-lipid suspensions containing PEG-2000 (Fig. 1, C and E) or PEG-5000 (Fig. 1 D and F), one repeat period was equal to that of DSPC bilayers at the same applied pressure and the second repeat period had a value similar to that recorded for the DSPC:PEG-lipid suspensions at a higher PEG-lipid concentration, indicating phase separation between a DSPC phase and a DSPC:PEG-lipid phase. For DSPC:PEG-lipid suspensions containing 20 mol % of PEG-750 (Fig. 1 B), one repeat period was 15–20 Å larger than the other, indicating phase separation between DSPC:PEG-lipid bilayers in the LβI phase and Lβ' phase.

The lamellar repeat period contains contributions from both the phospholipid bilayer and the fluid space between adjacent bilayers. To determine the width of the phospholipid bilayer (d_b) and the fluid space (d_f) at each applied pressure we have used electron density profiles obtained from the lamellar diffraction data. In the accompanying paper (Kenworthy et al., 1995) we found that at low applied pressures

DSPC:PEG-lipid suspensions containing 0 to about 15 mol % PEG-lipid formed normal gel ($L\beta'$) phase bilayers for PEG-350, PEG-750, PEG-2000, and PEG-5000, and at higher concentrations of PEG-lipid, normal gel ($L\beta'$ or $L\beta$) phase bilayers were formed for DSPC:PEG-2000 and DSPC:PEG-5000, whereas gel bilayers with interdigitated hydrocarbon chains (the $L\beta I$ phase) were formed for DSPC:PEG-350 and DSPC:PEG-750. Here we consider the changes in bilayer structure in the range of osmotic pressures of $2 \times 10^3 < P < 1.6 \times 10^8$ dyn/cm^2 ($3.3 < \log P < 7.2$).

Fig. 2 shows typical electron density profiles for the $L\beta'$ phase at three applied pressures for DSPC containing 10 mol % PEG-5000. For each profile, a single unit cell is shown, with the middle of the bilayer centered at 0 Å. The low density trough in the center of each bilayer corresponds to the localization of the terminal methyl groups on the lipid hydrocarbon chains, the medium density regions on both sides of the terminal methyl trough correspond to the methylene groups of the hydrocarbon chains, and the high density peaks centered at ±25 Å correspond to the phospholipid head groups. The medium density regions beyond ±30 Å correspond to one-half the fluid space between adjacent bilayers, where the PEG chains are localized. For all of the profiles in Fig. 2, the portion of the profile corresponding to the phospholipid bilayer (from about −30 Å to +30 Å) was nearly the same for each applied pressure. Thus, both the wide-angle data and electron density profiles indicate that the $L\beta'$ phase bilayer structure remained approximately constant for applied pressures of 2×10^3-1.5×10^6 dyn/cm^2. However, the electron density profiles of Fig. 2 clearly show that the width of the space between bilayers decreased with increasing applied pressure.

Fig. 3 shows electron density profiles for the $L\beta I$ phase of PEG-350 at applied pressures of 1.06×10^5 and 2.81×10^6 dyn/cm^2. Again, for each profile a single unit cell is shown, with the middle of the bilayer centered at 0 Å. The low density region in the center of each bilayer corresponds to the hydrocarbon chain region of the bilayer. There is no terminal methyl trough, since the hydrocarbon chains from apposing

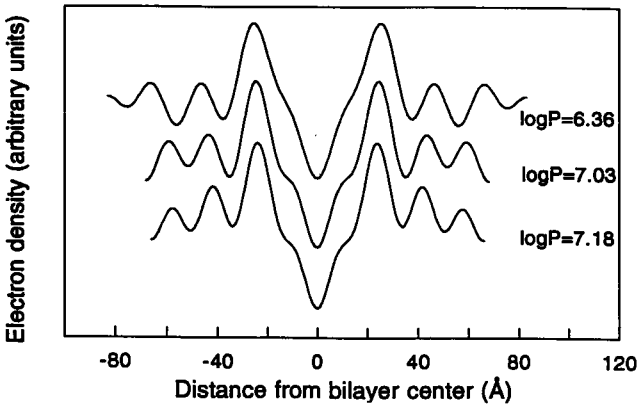

FIGURE 2 Electron density profiles of DSPC:PEG-5000 bilayers containing 10 mol % PEG-5000. The logarithms of the applied pressures are indicated on the figure.

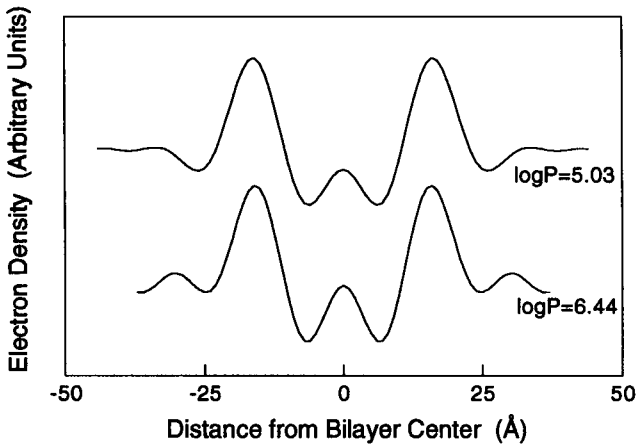

FIGURE 3 Electron density profiles of DSPC:PEG-lipid bilayers containing 100 mol % PEG-350. The logarithms of the applied pressures are indicated on the figure.

bilayers are interdigitated so that the terminal methyl groups are localized near the apposing hydrocarbon/water interfaces (McDaniel et al., 1983; McIntosh et al., 1983). The high density peaks centered at ±15 Å correspond to the phospholipid head groups and the medium density regions beyond the head group peaks correspond to the fluid spaces between bilayers. These profiles show that with increasing applied osmotic pressure the electron density distribution across the $L\beta I$ phase bilayers remained nearly constant, whereas the distance between apposing bilayers decreased.

The electron density profiles from DSPC:PEG-lipid bilayers in both the $L\beta'$ and $L\beta I$ phases were used to estimate the distance between adjacent bilayers (d_f). We used the same definition of phospholipid bilayer width (d_b) as we used in the preceding paper (Kenworthy et al., 1995) and in other papers (McIntosh and Simon, 1986; McIntosh et al., 1987, 1989a, b, 1992), where d_b is operationally defined as the total thickness of the phosphatidylcholine bilayer. As described in the previous paper (Kenworthy et al., 1995), we assumed d_b to be the distance between head group peaks (d_{pp}) in the profiles plus 10 Å, and for each applied pressure, the distance between bilayers was calculated from $d_f = d - d_b$.

A plot of the logarithm of applied pressure ($\log P$) versus d_f for DSPC bilayers and DSPC bilayers containing 5 mol % PEG-350, PEG-750, PEG-2000, and PEG-5000 is shown in Fig. 4. For applied pressures $2.5 < \log P < 6.5$, the distance between bilayers decreased monotonically with increasing applied pressure for each bilayer system. For each applied pressure, the distance between bilayers was a strong function of the size of the PEG-lipid, increasing with the size of the PEG-lipid. For PEG-2000 and PEG-5000 for high applied pressures ($\log P > 6.5$), two values of bilayer separation were observed, indicating lipid phase separation.

Plots of the logarithm of applied pressure versus d_f for DSPC:PEG-lipid suspensions containing various concentrations of PEG-350, PEG-750, PEG-2000, and PEG-5000, Avanti PEG-2000, and Avanti PEG-5000 are shown in Fig. 5, *A–F*, respectively. To simplify presentation of the data, we

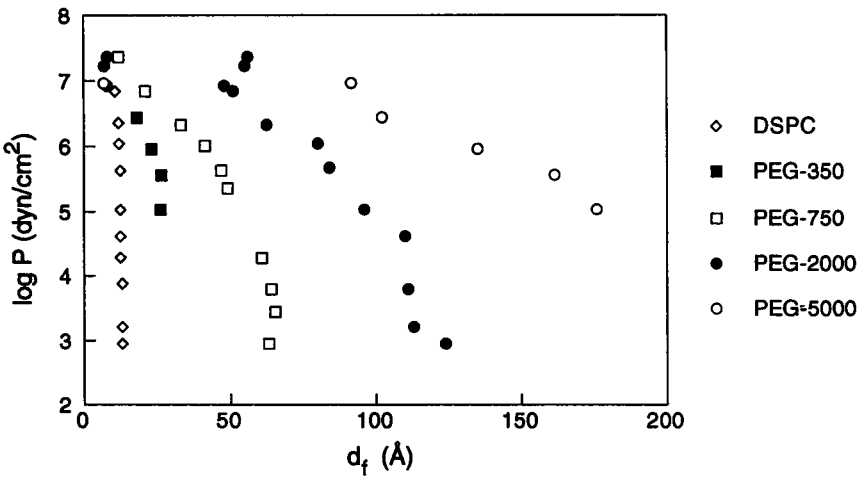

FIGURE 4 Logarithm of applied osmotic pressure versus distance between apposing bilayers for DSPC bilayers and DSPC bilayers containing 5 mol % PEG-350, PEG-750, PEG-2000, and Avanti PEG-5000.

do not present data where phase separation occurred. The log P-d_f relations depended strongly on both the PEG-lipid concentration and PEG molecular weight (Fig. 5). For DSPC: PEG-lipid suspensions in the Lβ' phase, for a given applied pressure the distance between bilayers increased with increasing PEG-lipid concentration until a limiting value was reached at a PEG-lipid concentration of about of 40 mol % for PEG-350 (Fig. 5 *A*) and 10 mol % for PEG-750 (Fig. 5 *B*), PEG-2000 (Fig. 5 *C*), Avanti PEG-2000 (Fig. 5 *D*), and PEG-5000 (Fig. 5 *E*), and 20 mol % for Avanti PEG-5000 (Fig. 5 *F*).

Several differences between the pressure-repeat period (Fig. 1) and pressure-bilayer separation relations (Fig. 5) should be noted. Although the pressure-repeat period curves were significantly different for DSPC:PEG-350 dispersions containing 100% PEG-350 and 20 mol % PEG-350 (Fig. 1 *A*), the pressure-bilayer separation curves for these concentrations (Fig. 5 *A*) were quite similar. This is because the differences in the pressure-repeat period curves were due to the difference in bilayer thickness for 100% PEG-350 (LβI phase) and 20 mol % PEG-350 (Lβ' phase). The same phenomenon was observed at applied pressures lower than 3×10^6 dyn/cm^2 for DSPC:PEG-750 dispersions containing 10 mol % PEG-750 (Lβ' phase) and 20 mol % PEG-750 (LβI phase). In that case also the differences in the pressure-repeat period data (Figure 1B) were due primarily to differences in bilayer thickness, so that the pressure-interbilayer separation curves were essentially identical (Fig. 5 *B*).

Comparisons of pressure-distance data from PEG-lipids obtained from Liposome Technology and Avanti Polar Lipids showed the following. For DSPC:PEG-2000, the log P-d_f data were similar for the two PEG-2000 samples (Fig. 5, *C* and *E*). However, for DSPC:PEG-5000 there were marked differences between the pressure-d_f relations for PEG-5000 from the two sources. In general, at a given applied pressure and a given PEG-lipid concentration, larger interbilayer spacings were observed for dispersions containing PEG-5000 from Avanti (Fig. 5 *F*) than from Liposome Technology (Fig. 5 *D*). As one specific example, at an applied pressure of log $P = 5$, DSPC with 5 mol % Avanti PEG-5000 gave an interbilayer spacing of about 170 Å (Fig. 5 *F*), whereas the same nominal concentration of Liposome Technology PEG-5000 gave an interbilayer spacing of about 130 Å (Fig. 5 *D*). These data mean that a given concentration of Avanti PEG-5000 gave a larger repulsive pressure than did the same nominal concentration of Liposome Technology PEG-5000. As noted previously (Kenworthy et al., 1995) these observed differences could be due to differences in either the relative purity, water content, or polymer molecular weight polydispersity of the Avanti and Liposome Tech PEG-lipid preparations. We have not pursued this question further.

Modeling of experimental results

Repulsive pressures

There are several possible nonspecific repulsive interactions that can operate between bilayers, including hydration pressure (LeNeveu et al., 1977; McIntosh and Simon, 1986; Rand and Parsegian, 1989), undulation pressure (Harbich and Helfrich, 1984; Evans and Parsegian, 1986), electrostatic pressure (Cowley et al., 1978; Israelachvili, 1991), and steric pressure from overlapping lipid head groups including the phospholipid head groups (McIntosh et al., 1987; Israelachvili and Wennerstrom, 1990; McIntosh and Simon, 1993) and the head groups containing covalently attached PEG (Needham et al., 1992a, b).

The hydration pressure should not contribute significantly to the pressures between PEG-lipid bilayers (Figs. 4 and 5), since the pressures between PEG-lipid bilayers have a much longer range (over 200 Å for PEG-5000) than the 10–15 Å range of the hydration pressure observed between phosphatidylcholine bilayers (McIntosh and Simon, 1986, 1993). Likewise, the steric pressure from overlapping phospholipid head groups is very short-ranged ($\approx$ 5 Å) (McIntosh et al., 1987; McIntosh and Simon, 1993) and should not contribute substantially to the observed pressure-distance relations. The contribution of undulation pressures should be essentially zero for these systems because only stiff, gel-phase bilayers were used in these experiments.

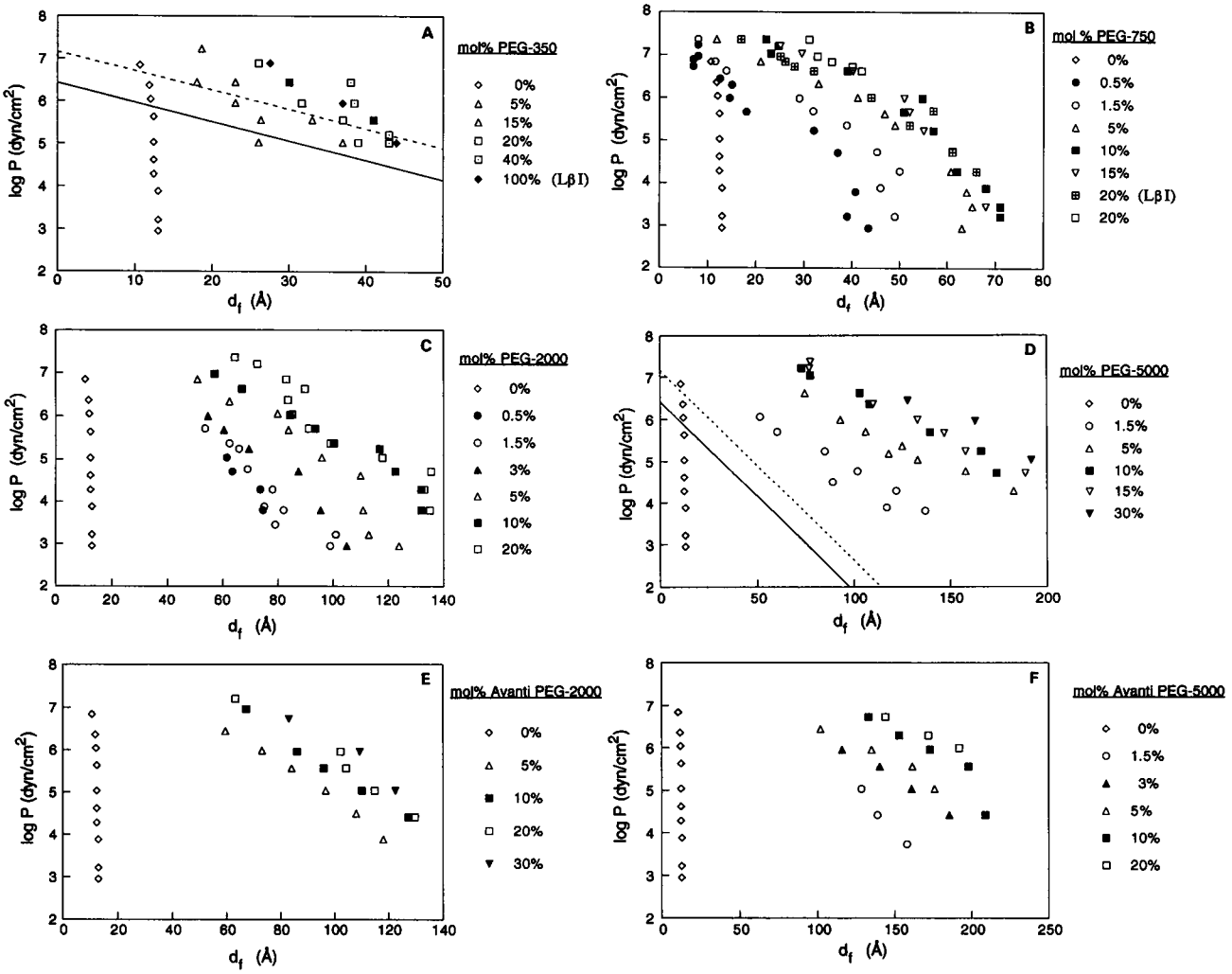

FIGURE 5 Logarithm of applied osmotic pressure versus distance between apposing bilayers for DSPC bilayers containing various concentrations of (*A*) PEG-350, (*B*) PEG-750, (*C*) PEG-2000, (*D*) PEG-5000, (*E*) Avanti PEG-2000, and (*F*) Avanti PEG-5000. Data points from bilayers in the interdigitated (LβI) phase are noted in panels (*A*) and (*B*). As described in the text, all other points are from bilayers in non-interdigitated phases (Lβ′ or Lβ). In panels (*A*) and (*D*) the predicted contributions of electrostatic repulsion (calculated from Eq. 2) are shown by solid and dotted lines for 5 and 15 mol % PEG-lipid, respectively.

The contribution of electrostatic repulsion to the total pressure for DSPC:PEG-lipid suspensions must be considered since Woodle et al. (1992a) showed that PEG-lipids have a negative charge localized to the ionized phosphate and Kuhl et al. (1994) demonstrated a long-range electrostatic repulsive interaction between bilayers containing PEG-2000. From classical double layer theory, the electrostatic repulsive pressure between two planar, charged surfaces at constant surface potential is given by

$$P_{es} = (64kT)c\gamma^2 \cdot \exp(-KD_{es}) \qquad (2)$$

where T is temperature, c is the bulk electrolyte concentration, $\gamma = \tanh(e\Psi_0/4kT)$ where Ψ_0 represents the membrane surface potential, K is the Debye length, and D_{es} is the distance between the planes where the charges are located (Israelachvili, 1991). Since the charge on the PEG-lipid is localized to the phosphate group, which is about 5 Å from the bilayer surface, we set $D_{es} = d_f + 10$ Å. For 0.1 M of 1:1 electrolytes, $K = 1/(9.6\text{ Å})$ and Ψ_0 can be evaluated from the Gouy equation

$$\sinh[e\Psi_0/(2kT)] = \sigma/(8N\epsilon\epsilon_0 kTc)^{1/2} \qquad (3)$$

where e is the electronic charge, k is the Boltzmann constant, T is the absolute temperature, σ is the surface charge density, N is Avogadro's number, ϵ is the dielectric constant, and ϵ_0 is the permittivity of free space (Eisenberg et al., 1979). To calculate σ, we use an area per molecule of 48 Å^2 for both DSPC and PEG-lipid and assume that all PEG-lipid molecules in the bilayer are charged. We make the simplifying assumption that the dielectric constant in the fluid space is the same as bulk water, although this assumption may not be strictly correct because of ordering of water molecules close to the bilayer surface and the presence of significant concentrations of PEG. The contributions of electrostatic repul-

sion predicted from Eq. 2 for various concentrations of PEG-lipid are shown in Fig. 5, *A* and *D*. These calculations show that the magnitude of electrostatic repulsion is comparable to the total pressures observed between DSPC:PEG-350 bilayers at values of d_f between 20 and 50 Å (Fig. 5 *A*), but very small compared with the observed repulsive pressures measured at the large values of d_f for DSPC:PEG-5000 (Fig. 5 *D*). Similar calculations show that the contribution of electrostatic repulsion to the total repulsion can be safely ignored for the ranges of pressures and d_f observed in all of our experiments with PEG-2000, Avanti PEG-2000, PEG-5000, and Avanti PEG-5000 (Fig. 5 *C–F*). However, electrostatic repulsion must be considered in analyzing the data from all DSPC:PEG-350 experiments and for experiments with DSPC:PEG-750 with PEG-750 concentrations >1.5 mol %.

Thus, based on these calculations, we argue that the data for DSPC:PEG-350 and DSPC:PEG-750 have contributions from both steric and electrostatic pressures, whereas over the range of pressures where we obtained discrete diffraction the primary repulsive pressure between DSPC:PEG-2000 and DSPC:PEG-5000 is steric repulsion between the apposed PEGs. We now analyze representative pressure-fluid space data with respect to theories for grafted-polymer interactions.

There are a number of theoretical treatments for the behavior of polymer chains grafted to surfaces (Alexander, 1977; deGennes, 1987, 1988; Milner, 1991; Milner et al., 1988b; Patel et al., 1988). These theories were initially developed for very long grafted polymers. Here we test whether the theories can predict the pressure-distance relations for surfaces with relatively short attached polymers. We note that Sarmoria and Blankschtein (1992) have performed Monte Carlo calculations that indicate that polymer scaling laws, such as those of deGennes (1988), are applicable for fairly short PEG chains (molecular weights greater than about 450 Da).

Definition of surface-grafted polymer regimes

According to deGennes (1987, 1988), two concentration regimes can be identified for the polymer chains at the surface. These two regimes, which have different physical characteristics, are referred to as "mushrooms" and "brushes". As shown schematically in Fig. 6, mushrooms form at low grafting densities where adjacent chains do not interact laterally, whereas brushes form at high grafting densities when adjacent chains overlap laterally. The definition of these regimes depends on both the distance between grafting sites (D) and the size of the random coil the polymer forms in solution, defined by the Flory dimension, $R_F = aN^{3/5}$, where N is the degree of polymerization and a is the monomer size or persistence length.

In the deGennes formalism (deGennes, 1987, 1988), the brush regime applies for $D < R_F$, and the mushroom regime applies for $D > R_F$. However, for the case of the mushroom regime, deGennes considered the case of a polymer grafted to only one of the apposed surfaces. In our experiments, PEGs are covalently attached to both apposing membranes. To apply the deGennes formalism to this geometry, we extend the theoretical treatment of the low grafting density mushroom regime by considering the effects of grafting density within that regime. Specifically, if the PEG mushrooms on the apposing bilayers were packed densely enough in the plane of the bilayer, then one would expect that apposing mushrooms would squeeze against one another when the apposing bilayers are brought together (Fig. 6, *middle panel*). However, if there were sufficiently large spaces between mushrooms in the plane of the bilayer, it could be possible that, upon compression, mushrooms from adjacent bilayers could squeeze past each other or interdigitate (Fig. 6, *left panel*). Thus, we further subdivide deGennes' low-grafting density ($D > R_F$) regime into two regimes, a "mushroom" regime for $2R_F > D > R_F$, where polymers from apposing bilayers interact at the midpoint between apposing bilayers, and an "interdigitated mushroom" regime for $D > 2R_F$, where polymers from apposing bilayers interdigitate.

To compare these theoretical parameters with those obtained experimentally, we set the persistence length $a = 3.5$ Å, the size of the chemical mer. Under this assumption, the values of N used in these calculations were obtained from $N = M_w/44$, where M_w is the weight-average molecular weight and 44 Da is the molecular weight of the mer

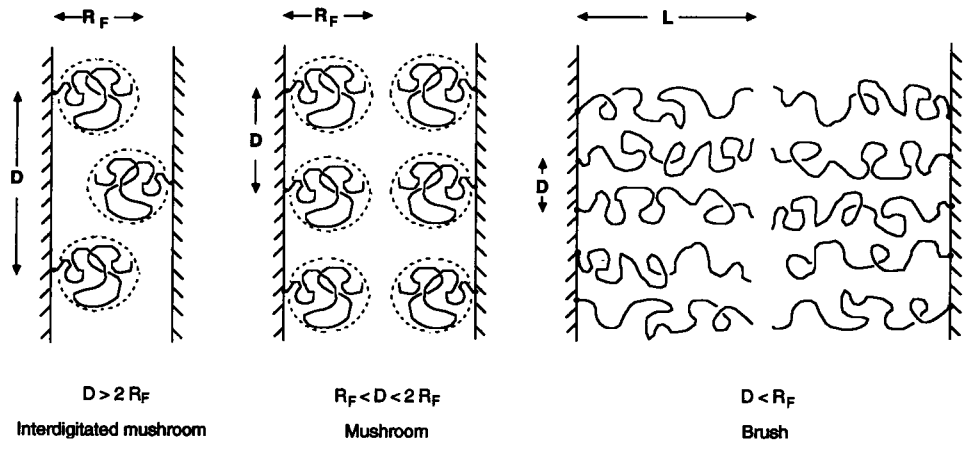

FIGURE 6 Schematic representation of surface-grafted polymer regimes: interdigitated mushrooms, mushrooms, and brushes. D represents the distance between PEG-lipids in the plane of the bilayer, R_F is the Flory dimension of the polymer in solution, and L represents the extension length of the polymer from the bilayer surface.

(CH_2—CH_2—O). In our experiments, D was calculated from the known mole fraction of PEG-lipid (M) and the area per lipid molecule in the bilayer A by $D = (A/M)^{1/2}$. The predicted regimes for DSPC:PEG-lipid specimens as a function of mol % PEG-lipid are shown in Fig. 7. The calculations predict that for DSPC:PEG-lipid bilayers, the conformation of PEG-750 is in either the interdigitated mushroom or mushroom regime for PEG-750 concentrations up to at least 14 mol %, whereas PEG-2000 and PEG-5000 both should form brushes over most of this concentration range.

Brief descriptions of the published formalisms, as modified by us for the geometry of the diffraction experiments, are given in Appendix 1. In addition to the deGennes formalisms, we also present a new Flory-based model for mushroom behavior designed to take into account the effects of small compressions on mushroom behavior (Hristova and Needham, 1994), and the mean-field parabolic brush model developed by Milner and colleagues (Milner, 1988, 1991; Milner et al., 1988b). Furthermore, in Appendix 2 we consider how the inherent polydispersity of the commercially available PEG should modify the theoretical predictions for each grafting regime.

Pressure-distance relations

We limit our theoretical analysis of grafted polymer pressure-distance behavior to the cases of PEG-750, PEG-2000, and PEG-5000. We do not attempt to model the steric interactions for DSPC:PEG-350 for two reasons: 1) electrostatic repulsion accounts for a major part of the observed repulsive pressure, and 2) it has been shown (Sarmoria and Blankschtein, 1992) that scaling laws only apply to PEG chains with >10 mers (molecular weight greater than about 450). Furthermore, we confine our analysis to the region of PEG-lipid concentrations where a single ($L\beta'$) phase was present, and thus the concentration of PEG-lipid in the bilayer was equal to the nominal concentration in the sample. For the case of PEG-5000, we model the pressure-distance results obtained for the high purity Avanti PEG-lipid.

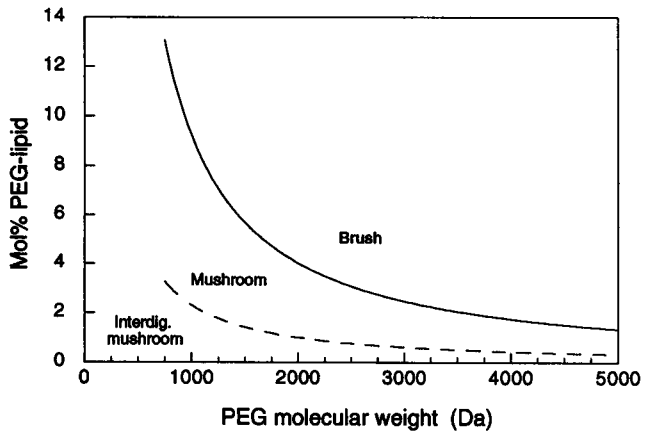

FIGURE 7 Putative PEG conformation regimes defined with respect to mol % PEG-lipid and nominal PEG molecular weights.

Comparisons of our experimental data and the various theoretical treatments for both monodisperse and polydisperse PEG molecular weight distributions are shown in Figs. 8–10 for various polymer lengths and grafting densities. Data sets were chosen so that the PEG-lipid molecular weights and concentrations were well within the boundaries of the three putative conformation regimes (Table 1): interdigitated mushrooms (Fig. 8), mushrooms (Fig. 9), and brushes (Fig. 10). Table 1 gives the R_F and D values for each of the test cases examined. In all of these calculations we have ignored the effects of the van der Waals attractive pressure.

Fig. 8 compares the experimental results for 1.5 mol % PEG-750 (Fig. 8, *A* and *B*) and 0.5% PEG-2000 (Fig. 8, *C* and *D*) with several theoretical predictions for mushrooms and interdigitated mushrooms. As shown in Fig. 8 A, for high applied pressures ($\log P > 6.5$) the 1.5 mol % PEG-750 data are well described by the Flory-based fully interdigitated mushroom models, but at lower applied pressures are underestimated by about 30 Å by either the monodisperse or polydisperse fully interdigitated mushroom models. As shown in Fig. 8 *B*, the model of partially interdigitated mushrooms, coupled with PEG molecular weight polydispersity, provides a reasonable description of the 1.5 mol % PEG-750 interbilayer spacings at pressures of $\log P = 6$ and below. Thus, for this data set, the fully interdigitated model fits the data best at high compressions ($\log P > 6.5$), whereas the non-interdigitated or partially interdigitated model fits best at low compressions ($\log P < 6.5$). Because of phase separation in the 0.5 mol % PEG-2000 samples no data were available to compare with the theoretical predictions at applied pressures $\log P > 5.5$ (Fig. 8, *C* and *D*). At low applied pressures, even when polydispersity effects are taken into account, the fully interdigitated mushroom model greatly underestimates the measured bilayer separations (Fig. 8 *C*). Under the conditions of these experiments, the data are approximately equally well described by either the non-interdigitated or partially interdigitated mushroom models in either the presence or absence of polymer molecular weight polydispersity (Fig. 8 *D*).

Fig. 9 shows comparisons of the predictions of the non-interdigitated mushroom models with the experimental results for 10 mol % PEG-750 (Fig. 9 *A*) and 3 mol % PEG-2000 (Fig. 9 *B*). As shown in Fig. 9 *A*, at pressures of $\log P > 7$, either the deGennes or the Flory-based monodisperse mushroom models describe the PEG-750 data within the limits of experimental scatter, but at lower applied pressures the experimental bilayer separations are up to 30 Å larger than predicted by either model. However, as shown in Fig. 9 *A*, the contribution of electrostatic repulsion accounts for these bilayer separations at pressures of $\log P < 4.5$. The remaining shortfall between the measured and predicted fluid spaces at applied pressures between $\log P = 4.5$ and 6.5 can be at least partially accounted for by the expected contribution of PEG polydispersity effects (Fig. 9 *A*). As shown in Fig. 9 *B*, the measured interbilayer spacings for 3 mol % PEG-2000 are somewhat (up to 10 Å) smaller than predicted for either the deGennes and Flory-based monodisperse mushroom models

TABLE 1 PEG conformations and interbilayer spacings for selected PEG-lipid samples*

PEG-lipid	R_F (Å)	D (Å)	Regime	d_f (Å) Theory: Monodisperse	d_f (Å) Theory: Polydisperse	d_f (Å) Experiment
1.5 mol % PEG-750	19.2	56.6	Interdigitated mushroom	19.2, 38.4	26, 50	49
10 mol % PEG-750	19.2	21.9	Mushroom	38.4	46	57
0.5 mol % PEG-2000	36.6	98.0	Interdigitated mushroom	36.6, 73.2	45, 83	75
3 mol % PEG-2000	36.6	40.0	Mushroom	73.2	97	105
10 mol % PEG-2000	36.6	21.9	Brush	103	116	132
5 mol % PEG-5000	64.0	31.0	Brush	200	220	176

*Values for d_f, taken from Figs. 8–10, are for the lowest applied pressure shown, except for 10 mol % PEG 750, where log $P \sim 5$. The two theoretical values for interdigitated mushrooms are for full and partial interdigitation, respectively.

for $5 < \log P < 6$, whereas for $\log P < 5$ the experimental spacings are greatly underestimated by the theoretical values. However, here again the predicted effects of polydispersity in the mushroom regime help account for the interbilayer spacings observed for $\log P < 5$ (Fig. 9 *B*).

Fig. 10 shows comparisons of the experimental results for 10 mol % PEG-2000 (Fig. 10 *A*) and 5 mol % PEG-5000 (Fig. 10 *B*) with the predicted pressure-distance behavior for brushes. There is very good agreement between the 10 mol % PEG-2000 experimental data and the Milner monodisperse brush prediction for applied pressures for $5.5 < \log P < 6.5$; over this range of pressures, the deGennes model predicts slightly larger (~10 Å) extensions. For $\log P < 5.5$, the interbilayer spacings are up to 30 Å larger than predicted by either theory for monodisperse PEG chains. Fig. 10 *A* shows that the effect of PEG molecular weight polydispersity is in the right direction to account for the difference between the theoretical predictions and experimental results for $\log P < 5$, although the measured values are still up to 15 Å larger than expected for polydisperse PEG-2000 brushes). For bilayers containing 5 mol % Avanti PEG-5000, the theoretical interbilayer spacings are systematically larger than the experimental data at all applied pressures examined (Fig. 10 *B*). (A similar effect was observed for all Avanti PEG-5000 concentrations examined, data not shown.) Thus by including polymer polydispersity in the Milner brush calculations for the PEG-5000 brushes (Fig. 10 *B*), the agreement between the theoretical and experimental results becomes worse.

Maximum polymer extension length from bilayer surface

The theoretical treatments also predict the maximum extension length (Fig. 6) of the grafted polymer from the surface. In the deGennes (1988) analysis, the maximum extension length of the polymer is $L = R_F = a \cdot N^{3/5}$ in the case of mushrooms and $L = a \cdot N(a/D)^{2/3}$ in the case of brushes. These predicted extension lengths can be compared to our measured bilayer separations. For DSPC:PEG-2000 and DSPC:PEG-5000, where the repulsive interactions are purely steric, the maximum observed values of d_f at the lowest applied pressures (Fig. 5) provide estimates for the interbilayer distances where polymer chains from apposing bilayers first come into contact. For these cases L is approximately one-half the maximum value of d_f. In the case of DSPC:PEG-750 the maximum value of $d_f/2$ provides an upper estimate for the polymer extension length, since electrostatic interactions could increase $d_f/2$ beyond the length of the extended polymer. Measured and theoretical estimates for the maximum polymer extension length in terms of interbilayer spacings are given for various concentrations of PEG-lipid in Table 1. The theoretical values for extension length were calculated using deGennes' treatment for monodisperse mushrooms and brushes given in Appendix 1 and the theoretical treatment for the effects of PEG polydispersity given in Appendix 2.

In Fig. 11 we compare theoretical predictions for twice the maximum polymer extension length with our experimental estimates for the maximum fluid space (d_f) between bilayers for various DSPC:PEG-2000 suspensions as taken from Fig. 5 *C*. We use DSPC:PEG-2000 for this comparison, since all three putative polymer conformation regimes are predicted to occur with this system (Fig. 7). The deGennes theory for monodisperse polymer populations predicts that for the mushroom regime the maximum extension length should be independent of grafting density and be approximately equal to the R_F, whereas for the brush regime the maximum extension length ($L = a \cdot N(a/D)^{2/3}$) should increase with grafting density (Fig. 11, *dotted line*). This prediction gives a good estimate of the fluid space at the 0.5 mol % PEG-2000, but greatly underestimates the fluid spaces measured at higher PEG-2000 concentrations. The experimental data are also not consistent with this prediction in that the maximum fluid space between DSPC:PEG-2000 bilayers increases on going from 0.5 to 3 mol % PEG-2000, concentrations below the mushroom/brush border. However, both the inclusion of partial PEG interdigitation and the incorporation of polydispersity help to overcome this problem. In Fig. 11 the solid line shows the predicted extension lengths for partially interdigitated mushrooms, mushrooms, and brushes taking into account the effects of PEG polydispersity. It can be seen that the predicted effects of partial polymer interdigitation and polymer polydispersity generally improve the agreement between theory and experimental observation.

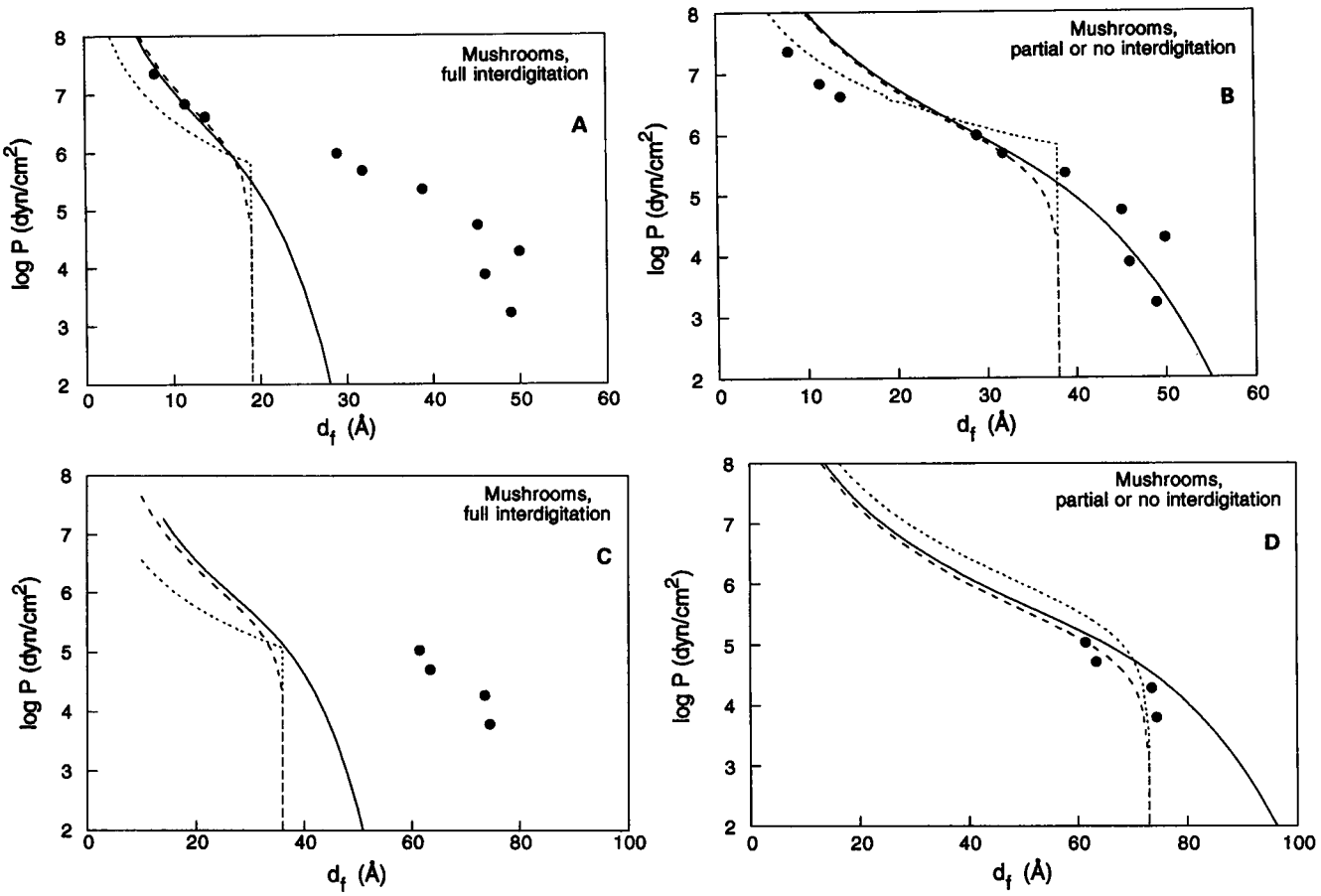

FIGURE 8 Experimental and theoretical results in the interdigitated mushroom regime. (*A*) Measured pressure-distance data for 1.5 mol % PEG-750 (●) compared with theoretical curves for fully interdigitated deGennes mushrooms (Eq. 4 with $h' = d_f$, truncated at $h' = R_F$) (·····), Flory-based predictions for fully interdigitating mushrooms (Eq. 5 with $h' = d_f$) (- - - -), and Flory-based predictions for polydisperse fully interdigitating mushrooms (Eq. 5, 12 with $h' = d_f$) (———). (*B*) Measured pressure-distance data for 1.5 mol % PEG-750 (●) compared with theoretical curves for deGennes mushrooms (Eq. 4 with $h' = d_f/2$, truncated at $h' = 2R_F$) (·····), Flory-based predictions for partially interdigitating mushrooms (Eq. 6) (- - - -), and Flory-based predictions for polydisperse partially interdigitated mushrooms (Eq. 6, 12) (———). (*C*) Measured pressure-distance data for 0.5% PEG-2000 (●) compared with theoretical curves for fully interdigitated deGennes mushrooms (Eq. 4 with $h' = d_f$, truncated at $h' = R_F$) (·····); Flory-based predictions for fully interdigitating mushrooms (Eq. 5 with $h' = d_f$) (- - - -), and Flory-based predictions for polydisperse fully interdigitating mushrooms (Eq. 5, 12 with $h' = d_f$) (———) (*D*) Measured pressure-distance data for 0.5% PEG-2000 (●) compared with theoretical curves for Flory-based predictions for partially interdigitating mushrooms (Eq. 6) (- - - -), Flory-based predictions for mushrooms (Eq. 5 with $h' = d_f$) (·····) and polydisperse partially interdigitated Flory mushrooms (Eqs. 6 and 12) (———).

DISCUSSION

PEG-lipid bilayer structure as a function of applied pressure

Over most of the range of applied pressures examined here, both the wide-angle diffraction and the electron density profile analysis show that the effects of applied pressure on bilayer structure were negligible. However, under some conditions, increasing applied pressure, and thus dehydrating the liposome, induced changes in the lipid structure. In the first instance, for DSPC:PEG-2000 and DSPC:PEG-5000 containing up to 10 mol % PEG lipid, phase separation between a pure DSPC phase and a PEG-lipid enriched DSPC:PEG lipid phase occurred at high applied pressures (log $P > 6$, Fig. 1, *C* and *D*). Similar phase separations at high applied pressures have been observed for other two-component bilayer systems (McIntosh et al., 1992). A second kind of phase change occurred for DSPC dispersions containing 20 mol % PEG-750, where, as the applied pressure was increased above $\sim 1 \times 10^6$ dyn/cm^2, the LβI phase that was observed in the absence of applied pressure was converted to a normal Lβ' gel phase (Fig. 1 *B*). This indicates that the formation of the Lβ' phase is favored at lower hydrations, consistent with similar observations of bilayers containing ether-linked phosphatidylcholine (Kim et al., 1987). A third shift in phase behavior with applied pressure was seen for DSPC:PEG-2000 containing 20 mol % PEG-2000, where compared to the curve for 10 mol % PEG-2000, the pressure-distance curve (Fig. 4 *C*) was shifted to relatively larger interbilayer separations at pressures above 1×10^6 dyn/cm^2. This may represent a shift from a mixed phase region containing micelles plus bilayers with a PEG-lipid concentration of about 10 mol

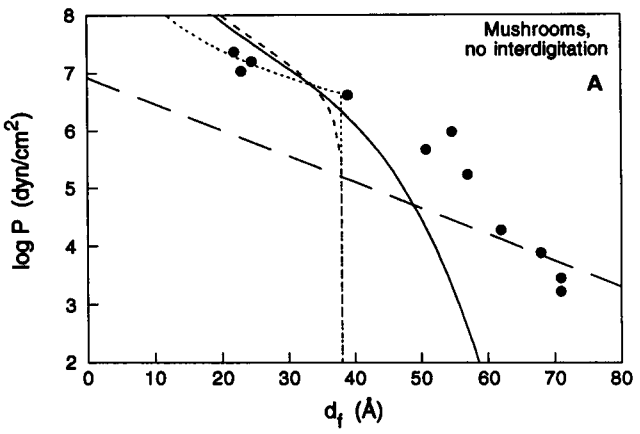

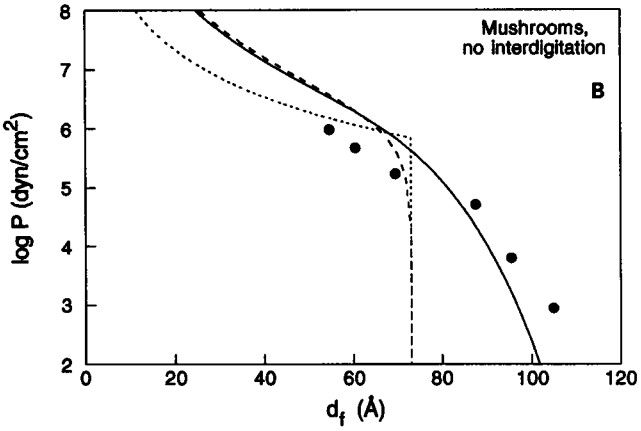

FIGURE 9 Experimental and theoretical results in the mushroom regime. (*A*) Measured pressure-distance data for 10 mol % PEG-750 (●) compared with theoretical predictions for deGennes mushrooms (Eq. 4 with $h' = d_f/2$) (·····), Flory mushrooms (Eq. 5 with $h' = d_f/2$) (- - - -), and polydisperse Flory mushrooms (Eq. 13) (———). Also shown is the predicted contribution of electrostatic repulsion (Eq. 2) (*large dashed line*). (*B*) Measured pressure-distance data for 3 mol % PEG-2000 (●) compared with theoretical predictions for deGennes mushrooms (Eq. 4 with $h' = d_f/2$) (·····, Flory mushrooms (Eq. 5 with $h' = d_f/2$) (- - - -), and polydisperse Flory mushrooms (Eq. 12) (———).

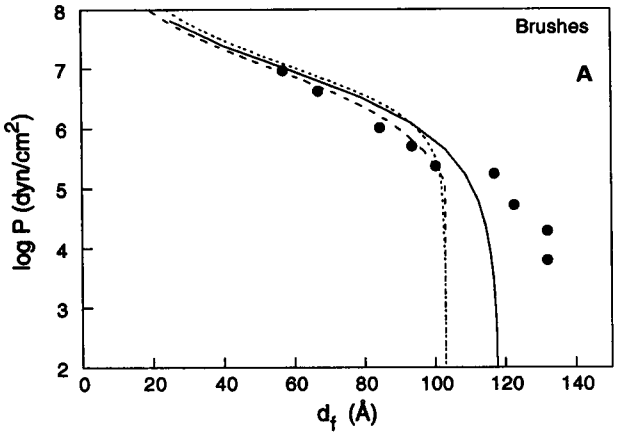

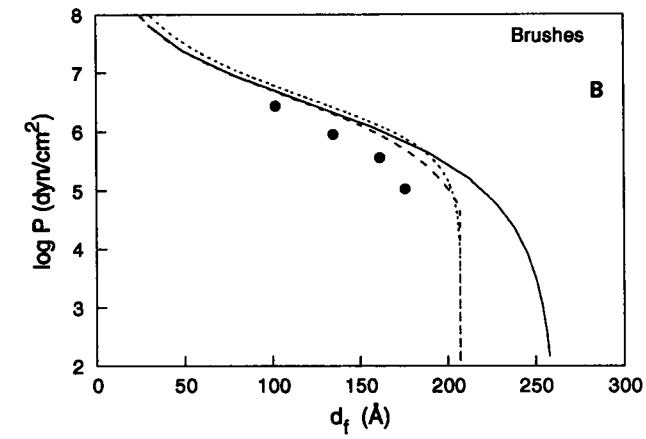

FIGURE 10 Experimental and theoretical results for the brush regime. (*A*) Measured pressure-distance data for 10 mol % PEG-2000 (●) compared with theoretical predictions for deGennes brushes (Eq. 7) (·····), Milner brushes (Eq. 8) (- - - -), and Milner polydisperse brushes (Eq. 12) (———). (*B*) Measured pressure-distance data for 5 mol % Avanti PEG-5000 (●) compared with theoretical predictions for deGennes brushes (Eq. 7) (·····), Milner brushes (Eq. 8) (- - - -), and Milner polydisperse brushes (Eqs. 13–15) (———).

%, the limiting concentration that can be incorporated at high hydrations (Kenworthy et al., 1995), to a pure bilayer phase containing about 20 mol % PEG-2000.

It is interesting to compare the pressure-distance relations for DSPC:PEG-750 dispersions containing 10 and 20 mol % PEG-750 (Fig. 5 *B*), two systems with very different bilayer structures but essentially identical grafting densities. DSPC with 10 mol % PEG-750 is in the Lβ' phase, whereas DSPC with 20 mol % PEG-750 is in the LβI phase, which has approximately twice the area per lipid molecule (Ranck et al., 1977; McIntosh et al., 1983). The observation that the interactive behaviors are similar for these two systems suggests that the behavior of the grafted PEG is independent of the bilayer "surface" to which the polymer is grafted.

Origin of the repulsive pressures between PEG-lipid bilayers

Our calculations indicate that, for the range of fluid spacings and pressures shown in Figs. 4 and 5, the interbilayer interactions in the DSPC:PEG-lipid system are dominated by electrostatic repulsion for PEG-350, steric interactions for PEG-2000, and PEG-5000, and a combination of electrostatic and steric interactions for PEG-750. In terms of electrostatic pressures, it has previously been shown by comparing pressure-distance data obtained at different ionic strengths that, for the range of fluid spacings shown in Figs. 4 and 5, electrostatic repulsion is small compared with steric repulsion for phosphatidylcholine bilayers containing 4 mol % PEG-2000 (Needham et al., 1992). However, for all the PEG-lipid bilayers electrostatic repulsion may be important at larger fluid separations, as shown directly by pressure-distance relationships measured by Kuhl et al. (1994), who argue that at low applied pressures and large fluid separations in the range of 200 to 600 Å, their pressure-distance data could be explained solely by electrostatic repulsion. At smaller separations, upward deviations in the pressure-distance relations were interpreted in terms of the onset of steric pressures between bilayers (Kuhl et al., 1994). In our experiments for PEG-2000 and PEG-5000, the pressure-distance data are obtained over the range of applied pressures

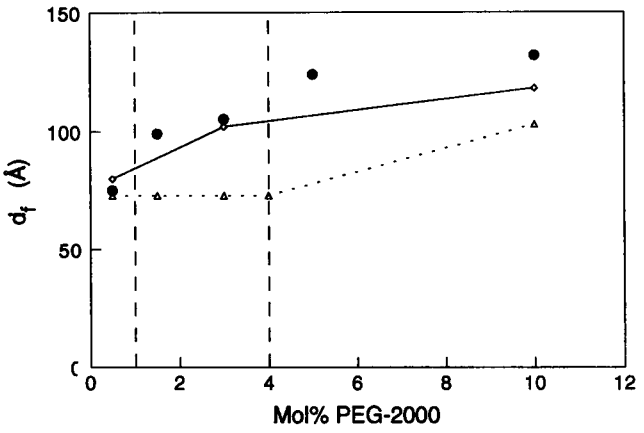

FIGURE 11 Experimental values (●) and theoretical predictions for the distance between bilayers for DSPC:PEG-2000 liposomes as a function of PEG-2000 concentration. The dotted line represents predictions based on deGennes' theory for the mushroom and brush regime, and the solid line represents the predictions for the partially interdigitated mushroom, mushroom, and brush regimes taking into account the effects of polydispersity (see Appendices 1 and 2). The boundaries between the putative polymer regimes are indicated by the dashed horizontal lines; the interdigitated mushroom regime extends from 0 to 1 mol % PEG-2000, the mushroom regime extends from 1 to 4 mol %, and the brush regime is formed for concentrations >4 mol % PEG-2000 (see Fig. 7).

and interbilayer spacings where steric pressures dominate. In the absence of applied pressure, our DSPC:PEG-liposomes produced broad diffraction bands (Kenworthy et al., 1995), indicating that the liposomes had large interbilayer fluid spaces, consistent with the presence of long-range electrostatic repulsion.

Comparison of pressure-distance data to other grafted polymers experiments

In the past several years the surface force apparatus has been used to measure the interactions in various solvents between mica surfaces with several types of attached polymers (Klein and Luckham, 1982, 1984; Luckham and Klein, 1985; Claesson and Gölander, 1987; Taunton et al., 1988a,b; Marra and Hair, 1988; Patel and Tirrell, 1989; Klein, 1990; Costello et al., 1992, 1993; Watanabe and Tirrell, 1993). Here, we restrict our attention to studies using water as the solvent and attached PEGs with chains lengths comparable to those used in our studies. Two groups have analyzed the forces between mica surfaces with low molecular weight PEGs (referred to in those papers as polyethylene oxides or PEOs) attached to the surface via a molecular anchor. Claesson and Gölander (1987) investigated an electrostatically anchored polyethylene oxide ester of lysine with the PEO chain having a molecular weight of about 1900, and Costello et al. (1993) studied copolymers of PEO and polymethyl methacrylate (PMMA) with PEO molecular weights of 750 and 2000. Both groups found that at large surface separations their pressure-distance relations could be accounted for by electrostatic repulsion between the charged mica plates. However, as the mica sheets were brought together upward breaks in the pressure-distance relations were ascribed to the onset of steric forces. In the case of PEO-lysine, the upward break was quite sharp and occurred at about 100 Å, whereas for PEO-PMMA for PEO molecular weights of both 750 and 2000 the upward breaks were rather broad and occurred at a mica sheet separation of about 200 Å. These results can be compared with our pressure-distance relations for DSPC:PEG-2000, where the steric pressure extended to an interbilayer separation of between 100 and 150 Å (Fig. 5 *C*), depending on the mole ratio of PEG-2000 incorporated into the bilayer, or for DSPC:PEG-750, where the steric pressure extended to an interbilayer separation of between 50 to 75 Å, depending on the mole ratio of PEG-750 incorporated into the bilayer (Fig. 5 *B*). Thus, there is reasonable agreement in terms of polymer extension length among the measurements for PEG-2000, especially if one assumes that the observed differences are due to the unknown grafting density in the surface force apparatus experiments.

Kuhl et al. (1994) used the surface force apparatus to measure the interactions between distearoylphosphatidylethanolamine bilayers containing three different concentrations of PEG-2000. As noted above, they observed long-range exponential decays for all three systems that could be explained by electrostatic repulsion. As apposing bilayers were brought together, upward breaks were observed in the pressure-distance relations which were ascribed to the onset of steric pressure. These breaks occurred at interbilayer separations of 70–80 Å for 1.3 mol % and 4.5 mol % PEG-2000 and at 140–150 Å for 9.0 mol % PEG-2000. The surface force apparatus value for 9 mol % is in excellent agreement with our observed pressure-distance relation (Fig. 5 *C*), whereas the surface force apparatus values for 1.3 and 4.5 mol % PEG-2000 are somewhat smaller than our observed maximum value of d_f at similar PEG-2000 concentrations (Fig. 5 *C*).

Comparison of data to theoretical predictions

The pressure-distance relations arising from the PEG of the PEG-lipid incorporated in DSPC bilayers are presented as a function of polymer conformation–interdigitated mushrooms, mushrooms, and brushes–predicted by several different formalisms, including those by deGennes (1976, 1980, 1985, 1987), by Milner and colleagues (Milner et al., 1988a,b, 1989; Milner, 1991), and a more recent approach based on Flory's mean-field arguments by Hristova and Needham (1994).

Mushrooms: full, partial, and no polymer interdigitation

Based on simple geometric considerations (Fig. 6), we argue that the mushroom regime can be broken down further into two distinct sub-regimes, "mushrooms" where $R_F < D < 2R_F$, and "interdigitated mushrooms" where $D > 2R_F$. We further hypothesize that within the interdigitated mushroom regime, at least two possible kinds of interactions could occur: 1) full interdigitation and 2) partial interdigitation, where the degree

of interdigitation depends on surface coverage and compression (applied pressure).

Comparisons of pressure-distance data and theoretical predictions (Fig. 8 *A* and *C*) show that full interdigitation does not occur at low compressions (low applied pressures, log $P < 6$), even under circumstances ($D > 2R_F$) where there should be enough space for the mushrooms to interdigitate to relax the compressive load. Moreover, for 0.5% PEG-2000 polymer extensions at low pressures are close to those predicted for partially interdigitated mushrooms or non-interdigitated mushrooms (Fig. 11). That full interdigitation does not occur at low compressions is probably due to the fact that "trapping" the mushrooms grafted to one surface in the free space between the mushrooms on the apposing surface would decrease the entropy of the system. However, at high compression (log $P > 6$), the theoretical treatment for fully interdigitated mushrooms describes the data better than the predictions for mushrooms or partially interdigitated mushrooms (Fig. 8 *A*). Thus, it appears that the degree of polymer interdigitation depends on the amount of applied pressure.

For grafting densities in the non-interdigitated mushroom regime ($D > R_F$) at low applied pressures (log $P < 6$), the experimental interbilayer spacings were generally significantly larger than predicted by either the deGennes or Flory-based grafted polymer theories for monodisperse PEG mushrooms (Fig. 9 and 11). (Our experimental data could not distinguish between these two theoretical treatments, since both give similar predictions at low applied pressures, and, because of phase separation, we could not obtain many data points at the high applied pressures where the two treatments differ.) The incorporation of polydispersity in the Flory-based mushroom models worked to improve the agreement between theory and experiment for all the putative "mushrooms" examined under conditions of low applied pressure (Figs. 9 *B* and 11). However, polydispersity is predicted to have little effect at high applied pressures.

Brushes

Polymer brushes are the best understood and most studied regime of grafted polymer interactions. In the brush regime, the deGennes theory predicts that, because of lateral interactions between grafted polymers, the extension length of the polymer from the surface (L) should be greater than the Flory dimension (R_F) of the polymer in solution. Our experimental data for maximum polymer extension length ($d_f/2$ for the brush regime in Table 1) are in clear support of that prediction.

In terms of the pressure-distance data, for monodisperse brushes there is little difference in the behavior predicted for deGennes and Milner brushes over the range of our experiments (Fig. 10). However, the relationship between the experimental pressure-distance data and the theoretical predictions differed for the PEG-2000 and PEG-5000 brushes. By use of the Milner equations to include the polydispersity of the PEG-2000, the theoretical prediction for 10 mol % PEG 2000 data (Fig. 10 *A*) was improved somewhat at low compressions (although it still underestimated the observed interbilayer spacings), whereas the discrepancy between the observed and predicted interbilayer spacings in the 5 mol % PEG-5000 system increased (Fig. 10 *B*). It is presently unclear why the relationship between the data and theoretical brush predictions differed between these two experimental systems.

Thus, the combination of established (deGennes, 1976, 1985, 1988; Milner, 1988; Milner et al., 1988a,b) and more recent (Hristova and Needham, 1994) theories presented in this paper gives a reasonable description of the x-ray diffraction data at high compressions if PEG polydispersity is taken into account, even under the simple assumption that the persistence length a is equal to the chemical mer size.

Implications for liposomal drug delivery

In the accompanying paper (Kenworthy et al., 1995), we showed that, for a single applied pressure, the spacings between DSPC:PEG lipid bilayers increase with PEG molecular weight and PEG-lipid concentrations up to about 10 mol %, in agreement with the steric barrier model for the increased blood circulation time of PEG-liposomes. Here, we find that both the magnitude and range of the steric barrier, and the compressibility of the PEG coat, are strong functions of PEG lipid concentration and PEG molecular weight (Figs. 4 and 5).

The pressure-fluid space curves (Figs. 4 and 5) also give estimates for twice the extension length of the PEG from the bilayer surface for a range of PEG molecular weights and PEG-lipid concentrations (Table 1). In addition to providing basic information about the minimum polymer extension necessary for effective steric barrier formation, such numbers may be useful for the design of "targeted" liposomes or other systems where it is of interest to incorporate into the liposomes other molecules that extend away from the liposome surface, such as antibodies or biotinylated lipids. For targeted liposomes, for instance it might be important for the targeting molecule to have access to the surroundings and not be completely covered by the PEG (Klibanov et al., 1991; Blume et al., 1993).

We also raise the possibility that a key factor in determining the effectiveness of the PEG steric barrier might be the relative surface coverage of the polymer. Thus, we predict that concentrations and sizes of PEGs should be selected to insure that the grafted polymers are in the brush regime, rather than in the mushroom regime. The brush regime is defined with respect to the point at which lateral interactions occur between neighboring PEGs, implying total coverage of the liposome surface with "overlapping" polymer chain. This may be a reason that 7.5 mol % PEG-2000 and PEG-5000 (both in the brush regime) effectively extend the blood circulation time of liposomes, whereas 7.5 mol % PEG-750 (mushroom regime) does not (Woodle et al., 1992b).

We thank Dr. Sidney Simon for many helpful discussions during the course of this work. We also thank Dr. D. Lasic of Liposome Technology, Inc., for supplying us with the PEG-lipids.

This work was supported by grant GM-27278 from the National Institutes of Health.

APPENDIX 1

Theoretical treatments for grafted polymer interactions

When two apposing PEG-lipid bilayers are made to approach each other under applied osmotic pressures, as in our x-ray diffraction experiments, the pressure-versus-distance profiles that characterize the polymer compressibility are dependent on surface concentration and hence on the regime. Here we consider the theoretical treatments that have previously been presented for both the brush and mushroom regimes, and describe how we have applied these treatments to compare the theoretical predictions with our experimental data.

Mushroom regime

The repulsive pressure of polymer mushrooms compressed between two parallel solid plates was first characterized by deGennes (1987, 1988). DeGennes considered the case of polymers attached to a single plate, where the repulsive interaction appears first at a critical interplate distance of $h' \approx R_F$. For strong compression, when the distance between the plates $h' \ll R_F$, the pressure is given by deGennes (1987, 1988) as:

$$P_{conf}(h') = (kTN/aD^2) \cdot (a/h')^{8/3} \quad (4)$$

To be able to interpret the x-ray diffraction data at all applied pressures, it is important to know the confinement energy at small compressions, when $h' \approx R_F$. Using Flory's mean-field arguments, Hristova and Needham (1994) have proposed that in the case where mushrooms are compressed such that $h' \leq R_F$, the system responds with a pressure

$$P_{mf}(h') = (kTN^{1/5}/D^2) \cdot (R_F^3/h'^4 - h'/R_F^2) \quad (5)$$

DeGennes considered the case of a polymer grafted to only one of the apposed surfaces, but in our experiments, PEGs are covalently attached to apposing membranes. To apply the deGennes formalism to this geometry, we extend the theoretical treatment of the mushroom regime by considering the effects of grafting density within the mushroom regime and the effects of large and small compressions on mushroom behavior. Specifically, if $2R_F > D > R_F$, the PEG mushrooms on the apposing bilayers are packed densely enough in the plane of the bilayer that they can squeeze against one another when these apposing bilayers are brought together (Fig. 6). At low compressions, when the apposing mushrooms first come into contact, the interaction should be most appropriately described using Eq. 5 with the distance between bilayers $h' = d_f/2$. When these apposing mushrooms are more highly compressed, it is more appropriate to apply the deGennes formalism using Eq. 4 with the distance between bilayers $h' = d_f/2$.

Interdigitated mushroom regime

In the case of DSPC:PEG-lipid bilayers containing very low concentrations of PEG-lipids, we consider an additional regime. That is, if $D > 2R_F$, the bilayers are so sparsely covered by polymer that when apposing bilayers approach, a mushroom grafted to one bilayer might be compressed directly against the apposing bilayer. That is, the mushrooms from opposite bilayers might interdigitate, as shown schematically in Fig. 6. At least two types of interdigitation are possible, full or partial interdigitation. In the first case, full interdigitation, each mushroom is compressed between two plates of separation h', similar to the situation described by deGennes (1987, 1988). Then the pressure is described by Eq. 4 with $h' = d_f$. The second, and more general case, is that of partial or surface-coverage dependent interdigitation. In this case, although there is enough space for the mushrooms to interdigitate, two apposed mushrooms can also be compressed against one another with a probability that is proportional to the surface coverage. By making the (initial) simplifying assumption that the mushrooms do not move on the surface, we calculate that two mushrooms will interdigitate with probability $(D - R_F)/D$ so that the average pressure is given by

$$P_{int}(d_f) = \{(D - R_F)/D\}P_{mf}(d_f) + \{R_F/D\}P_{mf}(d_f/2) \quad (6)$$

where the term P_{mf} is given by Eq. 5. Note that the pressure-distance relationship between mushrooms (Eq. 5) is steeper than that predicted here for interdigitated mushrooms. The assumption that the mushrooms are immobile is true if lipid diffusion in the plane of the bilayer does not occur. In gel phase lipid bilayers diffusion is present, although slow. The diffusion coefficient is of the order of 10^{-10} cm^2/s, so that in a 12-hour incubation period (typical for our x-ray samples) the average distance that a lipid would move is on the order of 30 μm. That means that over the course of the preparation of the x-ray samples the lipids would mix well. Therefore, there is a possibility for them to "slide" around each other and interdigitate; this may provide a way to "relax" the compressive pressures.

Brush regime

The repulsive pressures from compressed brushes have been described with both scaling and mean-field theories. In the scaling scheme (Alexander, 1977; deGennes, 1976, 1980, 1987, 1988) it is supposed that the mer concentration is constant throughout a polymer layer with thickness L. Alexander (1977) and deGennes (1976, 1980, 1987, 1988) consider the physical response of the polymer when two apposed brush-covered surfaces are brought into close contact. The pressure depends on the distance between surfaces (h) as

$$P_{sc}(h) = (kT/D^3) \cdot \{2L/h)^{9/4} - (h/2L)^{3/4}\} \quad (7)$$

where $L = Na(a/D)^{2/3}$. A mean field theory for dense brushes has been developed recently by Milner and colleagues (Milner, 1988, 1991; Milner et al., 1988a,b). Their analysis takes into account the possibility that the individual polymer chains may not be uniformly stretched, so that the mer concentration varies throughout the polymer layer. They show that the self-similar concentration varies throughout the polymer layer. They show that the self-similar concentration profile of this brush is parabolic, and, as a result, the mean-field brush is "softer" upon compression than predicted by scaling arguments. However, these mean-field arguments give pressure relationships with exponents close to the ones obtained by Alexander and deGennes. The mean-field theory of Milner and colleagues (Milner, 1988, 1991; Milner et al., 1988a,b) represents the repulsive pressure as

$$P_{MWC}(h) = P_o\{Lo/(h/2)^2 - h/L_o^2 + (h/2)^4/(L_o)^5\} \quad (8)$$

where $P_o = (kTN/2)\{\pi^2/12)^{1/3}a^{4/3}/D^{10/3}$ and $L_o = (12/\pi^2)^{1/3} \cdot N(a)^{5/3}/D^{2/3}$.

In the case of brushes, the deGennes and Milner-Witten-Cates formalisms (Milner et al., 1988a,b, 1989) can be compared to the x-ray data by equating the distance between grafting surfaces, h in Eqs. 7 and 8, to the distance between bilayer surfaces, d_f.

APPENDIX 2

Predicted effects of PEG polydispersity

The index of polydispersity is given by M_w/M_n. Data provided by Union Carbide show that the polydispersity for typical preparations of PEG chains is close to Gaussian, so that the distribution of molecular weights can be modelled as

$$p(n) = 1/(2\pi)^{1/2}\sigma_G) \cdot \exp\{-(n - N_o)^2/2\sigma_G^2\} \quad (9)$$

where n is a variable referring to the numbers of mers per polymer, N_o is the mean, and σ_G is the variance. In terms of chemical mers, the parameters of the polydispersity are: PEG 750, $N_o = 17$ and $\sigma_G = 5$; PEG 2000, $N_o = 53$ and $\sigma_G = 11$; and PEG 5000, $N_o = 130$ and $\sigma_G = 20$. Note that N_o is the value for which the molecular distribution has its peak and is slightly different from N, the degree of polymerization corresponding to the weight average molecular weight.

Polydisperse mushrooms

In the mushroom regime, each polymer forms a separate coil and there are no steric interactions between the chains. Thus, each polymer will form a coil of different size. (This is only strictly true if there is no lateral diffusion in the bilayer. If diffusion is present the mushrooms can bump into each other. However, as shown elsewhere (Hristova and Needham, 1994), these lateral interactions are not likely to perturb the random coil of the mushrooms.) The compressing force for each mushroom then will be different and will depend on the chain length. Mathematically, the repulsive pressure for monodisperse mushrooms is described by Eq. 5 only for $d_f < 2R_F$. For $d_f > 2R_F$ the pressure should be 0, since the polymers grafted to opposite bilayers are not in contact. Thus the correct expression for the pressure as a function of d_f is given by

$$P_{mf}(d_f) = (kTN^{1/5}/D^2) \cdot (R_F^3/(d_f/2)^4 - (d_f/2)/R_F^2) \cdot (1 - \theta(d_f - 2R_F)) \quad (10)$$

or, since $R_F = aN^{3/5}$

$$P_{mf}(d_f) = (kT/D^2) \cdot (a^3N^2/(d_f/2)^4 - (d_f/2)/a^2N) \cdot (1 - \theta(d_f - 2R_F)) \quad (11)$$

where the theta function $\theta(x) = 1$ for $x > 0$ and $\theta(x) = 0$ for $x < 0$. Averaging over the molecular weight distribution (Eq. 9), we find the average pressure for polydisperse mushrooms to be:

$$P_{mf}(d_f) = kT/(D^2(2\pi)^{1/2}\sigma_G) \cdot \{a^3/(d_f/2)^4 \cdot \int N^2 \exp(-(N - N_o)^2/2\sigma_G^2) \cdot (1 - \theta(d_f - 2R_F))dN - (d_f/2)/a^2 \cdot \int \exp((-(N - N_o)^2/2\sigma_G^2) \cdot (1 - \theta(d_f - 2R_F))dN/N\} \quad (12)$$

In the case of partial interdigitation, the force is given by Eq. 6, using P_{mf} from Eq. 12.

Polydisperse brushes

In the brush regime, because of the cooperative behavior and the lateral interactions between the brushes, the characterization of the effects of polydispersity is not trivial. Milner et al. (1989) studied the effect of the polydispersity on brush properties. They suggested that the pressure-distance relation is governed by the following equations:

$$\sigma - \sigma(n) = (2^{5/2}/3\pi) \cdot \{(A(p) - U(n; p))^{3/2} + (3p^{1/2}/2^{1/2})(A(p) - U(n; p))^{1/2}\} \quad (13)$$

$$h/2(p) = 2^{3/2}/\pi \cdot \int (A(p) - U(n; p))^{1/2}dn \quad (14)$$

where $p = Pa^3/kT$ is the "dimensionless pressure", a^2/D^2 is the surface coverage, $\sigma(n)$ is the surface coverage for polymers of degree of polymerization less than n, n_{max} is the maximum number of mers in the largest chain, and $U(z)$ is a fictitious potential, mapping the polymer problem into a classical mechanical one. The zero of U is defined to be on the grafting surface, and U increases monotonically with increasing distance from the grafting surface until it reaches a maximum value at the outer edge of the brush, at a distance $h/2$ from the surface. We define $A = U(h/2)$. Knowing σ and $\sigma(n)$ and the applied pressure P one may solve Eq. 13 for $A(p) - U(n; p))$. After the numerical integration of Eq. 14, one obtains the distance h as a function of the pressure P. We extend this study to our case of a Gaussian distribution of polymer weights with mean N_o and variance σ_G. In that case

$$\sigma(n) = \sigma/((2\pi)^{1/2}\sigma_G) \cdot \int \exp\{(-(n' - N_o)^2/2\sigma_G^2\}dn' = \sigma/2(1 + \text{erf}(n - N_o/2^{1/2}\sigma_G)) \quad (15)$$

Using Eqs. 13 and 14 for $\sigma(n)$, we obtain the pressure-distance relations, again considering the persistence length $a = 3.5$ Å.

REFERENCES

Alexander, S. 1977. Adsorption of chain molecules with a polar head. A scaling description. *J. Phys. Paris.* 38:983–987.

Allen, T. M., A. K. Agrawal, I. Ahmad, C. B. Hansen, and S. Zalipsky. 1994. Antibody-mediated targeting of long-circulating (stealth) liposomes. *J. Liposome Res.* 4:1–26.

Allen, T. M., and C. Hansen. 1991. Pharmacokinetics of stealth versus conventional liposomes: effect of dose. *Biochim. Biophys. Acta.* 1068: 133–141.

Allen, T. M., C. Hansen, F. Martin, C. Redemann, and A. Yau-Young. 1991. Liposomes containing synthetic lipid derivatives of poly(ethyleneglycol) show prolonged circulation half-lives in vivo. *Biochim. Biophys. Acta.* 1066:29–36.

Blume, G., and G. Cevc. 1990. Liposomes for the sustained drug release in vivo. *Biochim. Biophys. Acta.* 1029:91–97.

Blume, G., and G. Cevc. 1992. Drug-carrier and stability properties of the long-lived lipid vesicles, cryptosomes, in vitro and in vivo. *J. Liposome Res.* 2:355–368.

Blume, G., G. Cevc, M. D. J. A. Crommelin, I. A. J. M. Bakker-Woudenberg, C. Kluft, and G. Storm. 1993. Specific targeting with poly-(ethylene glycol)-modified liposomes: coupling of homing devices to the ends of the polymeric chains combines effective target binding with long circulation times. *Biochim. Biophys. Acta.* 1149:180–184.

Claesson, P. M., and C.-G. Gölander. 1987. Direct measurements of steric interactions between mica surfaces covered with electrostatically bound low-molecular weight polyethylene oxide. *J. Colloid Interface Sci.* 117: 366–374.

Costello, B. A. deL., P. F. Luckham, and T. T. Tadros. 1992. Investigation of the interaction forces of polymer-coated surfaces using force balance, rheology, and osmotic pressure results. *Langmuir.* 8:464–468.

Costello, B. A. deL. P. F. Luckham, and T. F. Tadros. 1993. Forces between adsorbed low molecular weight graft copolymers. *J. Colloid Interface Sci.* 156:72–77.

Cowley, A. C., N. L. Fuller, R. P. Rand, and V. A. Parsegian. 1978. Measurement of repulsive forces between charged phospholipid bilayers. *Biochemistry.* 17:3163–3168.

deGennes, P. G. 1976. Scaling theory of polymer adsorption. *J. Phys. Paris.* 37:1445–1452.

deGennes, P. G. 1980. Conformation of polymers attached to an interface. *Macromolecules.* 13:1069–1075.

deGennes, P. G. 1985. Scaling concepts in polymer physics. Cornell University Press Ithaca, New York.

deGennes, P. G. 1987. Polymers at an interface: a simplified view. *Adv. Colloid Interface Sci.* 27:189–209.

deGennes, P. G. 1988. Model Polymers at interfaces. *In* Physical Basis of Cell-Cell Adhesion. P. Bongrand, editor. CRC Press, Boca Raton, Florida.

Eisenberg, M., T. Gresalfi, T. Riccio, and S. A. McLaughlin. 1979. Adsorption of monovalent cations to bilayer membranes containing negative phospholipids. *Biochemistry* 18:5213–5223.

Evans, E. A. and V. A. Parsegian. 1986. Thermal-mechanical fluctuations enhance repulsion between bimolecular layers. *Proc. Nat. Acad. Sci. USA.* 83:7132–7136.

Gabizon, A. A. 1992. Selective tumor localization and improved therapeutic index of anthracyclines encapsulated in long-circulating liposomes. *Cancer Res.* 52:891–896.

Harbich, W., and W. Helfrich. 1984. The swelling of egg lecithin in water. *Chem. Phys. Lipids.* 36:39–63.

Hristova, K., and D. Needham. 1994. The influence of polymer-grafted lipids on the physical properties of lipid bilayers: a theoretical study. *J. Colloid Interface Sci.* 168:302–314.

Israelachvili, J. N. 1991. Intermolecular and surface forces. Academic Press, London. 221–245.

Israelachvili, J. N., and H. Wennerstrom. 1990. Hydration or steric forces between amphiphilic surfaces? *Langmuir.* 6:873–876.

Kenworthy, A. K., S. A. Simon, and T. J. McIntosh. 1995. Structure and phase behavior of lipid suspensions containing phospholipids with covalently attached poly(ethylene glycol). *Biophys. J.* This issue.

Kim, J. T., J. Mattai, and G. G. Shipley. 1987. Gel phase polymorphism in ether-linked DHPC bilayers. *Biochemistry.* 26:6592–6598.

Klein, J. 1990. Forces between polymer-bearing surfaces: the question of constrained equilibrium. *J. Phys.: Condensed Matter.* 2:SA323–SA328.

Klein, J., and P. Luckham. 1982. Forces between two adsorbed polyethylene oxide layers immersed in a good aqueous solvent. *Nature.* 300:429–430.

Klein, J., and P. F. Luckham. 1984. Forces between two adsorbed poly(ethylene oxide) layers in a good aqueous solvent in the range 0–150 nm. *Macromolecules.* 17:1041–1048.

Klibanov, A. L., K. Maruyama, A. M. Beckerleg, V. P. Torchilin and L. Huang. 1991. Activity of amphipathic poly(ethylene glycol) 5000 to prolong the circulation time of liposomes depends on the liposome size and is unfavorable for immunoliposomes binding to target. *Biochim. Biophys. Acta.* 1062:142–148.

Klibanov, A. L., K. Maruyama, V. P. Torchilin, and L. Huang. 1990. Amphipathic polyethylene glycols effectively prolong the circulation time of liposomes. *FEBS Lett.* 268:235–237.

Kuhl, T. L., D. E. Leckband, D. D. Lasic, and J. N. Israelachvili. 1994. Modulation of interaction forces between bilayers exposing short-chained ethylene oxide headgroups. *Biophys. J.* 66:1479–1488.

Lasic, D. D., F. J. Martin, A. Gabizon, S. K. Huang and D. Papahadjopoulos. 1991. Sterically stabilized liposomes: a hypothesis on the molecular origin of the extended circulation times. *Biochim. Biophys. Acta.* 1070: 187–192.

LeNeveu, D. M., R. P. Rand, V. A. Parsegian, and D. Gingell. 1977. Measurement and modification of forces between lecithin bilayers. *Biophys. J.* 18:209–230.

Luckham, P. F., and J. Klein. 1985. Interactions between smooth solid surfaces in solutions of adsorbing and nonadsorbing polymers in good solvent conditions. *Macromolecules.* 18:721–728.

Marra, J., and M. L. Hair. 1988. Surface forces between two layers of poly(ethyleneoxide) adsorbed from toluene on mica. *J. Colloid Interface Sci.* 125:552–560.

Mayhew, E. G., D. Lasic, S. Babbar, and F. J. Martin. 1992. Pharmacokinetics and antitumor activity of epirubicin encapsulated in long-circulating liposomes incorporating a polyethylene glycol-derivatized phospholipid. *Int. J. Cancer.* 51:302–309.

McDaniel, R. V., T. J. McIntosh, and S. A. Simon. 1983. Non-electrolyte substitution for water in lecithin bilayers. *Biochim. Biophys. Acta.* 731: 97–108.

McIntosh, T. J., A. D. Magid, and S. A. Simon. 1987. Steric repulsion between phosphatidylcholine bilayers. *Biochemistry.* 26:7325–7332.

McIntosh, T. J., A. D. Magid, and S. A. Simon. 1989a. Cholesterol modifies the short-range repulsive interactions between phosphatidylcholine membranes. *Biochemistry.* 28:17–25.

McIntosh, T. J., A. D. Magid, and S. A. Simon. 1989b. Range of the solvation pressure between lipid membranes: dependence on the packing density of solvent molecules. *Biochemistry.* 28:7904–7912.

McIntosh, T. J., R. V. McDaniel, and S. A. Simon. 1983. Induction of an interdigitated gel phase in fully hydrated lecithin bilayers. *Biochim. Biophys. Acta.* 731:109–114.

McIntosh, T. J., and S. A. Simon. 1986. The hydration force and bilayer deformation: a reevaluation. *Biochemistry.* 25:4058–4066.

McIntosh, T. J., and S. A. Simon. 1993. Contribution of hydration and steric (entropic) pressures to the interaction between phosphatidylcholine bilayers: experiments with the subgel phase. *Biochemistry.* 32:8374–8384.

McIntosh, T. J., S. A. Simon, D. Needham, and C.-H. Huang. 1992. Interbilayer interactions between sphingomyelin and sphingomyelin:cholesterol bilayers. *Biochemistry.* 31:2020–2024.

Milner, S. T. 1988. Compressing polymer brushes: a quantitative comparison of theory and experiment. *Europhys. Lett.* 7:695–699.

Milner, S. T. 1991. Polymer brushes. *Science.* 251:905–914.

Milner, S. T., T. A. Witten, and M. E. Cates. 1988a. A parabolic density profile for grafted polymers. *Europhys. Lett.* 5:413–418.

Milner, S. T., T. A. Witten, and M. E. Cates. 1988b. Theory of the grafted polymer brush. *Macromolecules.* 21:2610–2619.

Milner, S. T., T. A. Witten, and M. E. Cates. 1989. Effects of polydispersity in the end-grafted polymer brush. *Macromolecules.* 22:853–861.

Mori, A., A. L. Klibanov, V. P. Torchilin, and L. Huang. 1991. Influence of the steric barrier activity of amphipathic poly(ethyleneglycol) and ganglioside GM1 on the circulation time of liposomes and on the target binding of immunoliposomes in vivo. *FEBS Lett.* 284:263–266.

Needham, D., K. Hristova, T. J. McIntosh, M. Dewhirst, N. Wu, and D. D. Lasic. 1992a. Polymer-grafted liposomes: physical basis for the "stealth" property. *J. Liposome Res.* 2:411–430.

Needham, D., and T. J. McIntosh. 1991. Mechanical and interactive properties of lipid membranes containing surface-bound polymer: implications for liposome delivery design. *Biophys. J.* 59:500a.

Needham, D., T. J. McIntosh, and D. D. Lasic. 1992b. Repulsive interactions and mechanical stability of polymer-grafted lipid membranes. *Biochim. Biophys. Acta.* 1108:40–48.

Papahadjopoulos, D., T. M. Allen, A. Gabizon, E. Mayhew, K. Matthay, S. K. Huang, K.-D. Lee, M. C. Woodle, D. D. Lasic, C. Redemann, and F. J. Martin. 1991. Sterically stabilized liposomes: improvements in pharmacokinetics and antitumor therapeutic efficacy. *Proc. Nat. Acad. Sci. USA.* 88:11460–11464.

Parsegian, V. A., N. Fuller, and R. P. Rand. 1979. Measured work of deformation and repulsion of lecithin bilayers. *Proc. Nat. Acad. Sci. USA.* 76:2750–2754.

Parsegian, V. A., R. P. Rand, N. L. Fuller, and R. C. Rau. 1986. Osmotic stress for the direct measurement of intermolecular forces. *Methods Enzymol.* 127:400–416.

Patel, S., and M. Tirrell. 1989. Measurement of forces between surfaces in polymer fluids. *Annu. Rev. Phys. Chem.* 40:597–635.

Patel, S., M. Tirrell, and G. Hadziioannou. 1988. A simple model for forces between surfaces bearing grafted polymers applied to data on adsorbed block copolymers. *Colloid Surf.* 31:157–179.

Ranck, J. L., T. Keira, and V. Luzzati. 1977. A novel packing of the hydrocarbon chains in lipids. The low temperature phase of DPPG. *Biochim. Biophys. Acta.* 488:432–441.

Rand, R. P., and V. A. Parsegian. 1989. Hydration forces between phospholipid bilayers. *Biochim. Biophys. Acta.* 988:351–376.

Sarmoria, C., and D. Blankschtein. 1992. Conformation characteristics of short poly(ethylene oxide) chains terminally attached to a wall and free in aqueous solution. *J. Phys. Chem.* 96:1978–1983.

Taunton, H. J., C. Toprakcioglu, L. J. Fetters, and J. Klein. 1988a. Forces between surfaces bearing terminally anchored polymer chains in good solvents. *Nature.* 332:712–714.

Taunton, H. J., C. Toprakcioglu, and J. Klein. 1988b. Direct measurement of the interaction between mica surfaces with adsorbed diblock copolymer in a good solvent. *Macromolecules.* 21:3336–3351.

Vink, H. 1971. Precision measurements of osmotic pressure in concentrated polymer solutions. *Eur. Polymer J.* 7:1411–1419.

Watanabe, H., and M. Tirrell. 1993. Measurement of forces in symmetric and asymmetric interactions between diblock copolymer layers adsorbed on mica. *Macromolecules.* 26:6455–6467.

Woodle, M. C., L. R. Collins, E. Sponsler, N. Kossovsky, D. Papahadjopoulos, and F. J. Martin. 1992a. Sterically stabilized liposomes. Reduction in electrophoretic mobility but not electrostatic surface potential. *Biophys. J.* 61:902–910.

Woodle, M. C., and D. D. Lasic. 1992. Sterically stabilized liposomes. *Biochim. Biophys. Acta.* 1113:171–199.

Woodle, M. C., K. K. Matthay, M. S. Newman, J. E. Hidayat, L. R. Collins, C. Redemann, F. J. Martin, and D. Papahadjopoulos. 1992b. Versatility in lipid compositions showing prolonged circulation with sterically stabilized liposomes. *Biochim. Biophys. Acta.* 1105:193–200.

Wu, N. Z., D. Da, T. L. Rudoll, D. Needham, and M. W. Dewhirst. 1993. Increased microvascular permeability contributes to preferential accumulation of stealth liposomes in tumor tissue. *Cancer Res.* 53:3765–3770.